

Micro-Flow Calibration Facility at NIST

James W. Schmidt: National Institute of Standards and Technology (NIST)

John D. Wright (NIST)

100 Bureau Drive, Gaithersburg, MD, USA 20899

Corresponding Author: jschmidt@nist.gov

Abstract

The Fluid Metrology Group (FMG) at the National Institute of Standards and Technology (NIST) is developing a primary, dynamic gravimetric liquid flow standard for use in the range 100 nL/min to 1 mL/min (and eventually lower). An elevated reservoir of water with a pressure head of a few centimeters provides a flow to the meter under test and the discharged water from it flows to a micro-balance. The flow is collected in a beaker which is weighed at intervals while it fills. The time-rate-of-change of the buoyancy-corrected mass of the beaker's contents gives the mass flow. The FMG's implementation of the flow standard will allow accurate measurements of non-steady flows and heterogeneous flows (liquids with cells, proteins, and other soluble and non-soluble components). Evaporation of the water from the beaker is a significant effect and must be measured or controlled accurately. Intermittent liquid wetting or "patchy" wettability of the pipette by the water in the beaker is also a significant effect. At present we are exploring two techniques: 1) using an oil film to limit evaporation, and 2) using a porous glass element to control capillary forces and evaporation losses. We present an uncertainty analysis for the first iteration of the flow standard. A preliminary calibration of a commercial flow meter was within 3 % or better down to 2 $\mu\text{L}/\text{min}$ of the unofficial calibrations conducted by the Danish and Swiss National Metrology Institutes.

1. Introduction

Drug delivery of minute quantities of powerful and often expensive drugs is becoming more prevalent. Diabetes for example is a common disease in the US that needs small, accurate quantities of insulin for treatment. Some forms of pain management require small doses of morphine sulfate whose rates of delivery should be controlled at the level of 30 nL/min [1,2]. Implantable micro pumps that can deliver liquid to the inner ear to ease symptoms of tinnitus are being developed [3]. Other pain medicines cost \$1000 per dose of 0.1 mL. Control and measurement of micro flows in the range 10 $\mu\text{L}/\text{min}$ and below is expected to become more important.

To accurately measure microflows, NIST's Fluid Metrology Group is establishing a Micro-Flow Calibration Facility to measure liquid flows in the range 1 mL/min down to 100 nL/min with 1 % uncertainty or better. At present we can measure flows over the range 100 $\mu\text{L}/\text{min}$ down to 1 $\mu\text{L}/\text{min}$ with an uncertainty of 5 %. In the remainder of this paper, we will describe: the apparatus, 1st iteration measurement and flow calibration techniques, results of experiments to quantify uncertainty components, and the results of a very informal comparison with the Danish Technological Institute (DTI) in Aarhus, Denmark, and the Swiss Federal Institute of Metrology (METAS) in Bern, Switzerland. Although the DTI and METAS calibrations were conducted on a very compressed time schedule and not following their normal calibration protocols (at our request), the DTI and METAS calibrations agreed within their specifications [4,5].

2. Micro-Flow Calibration Facility Apparatus

The apparatus consists of 1) a source of flow, 2) the flow meter or device under test (DUT), and 3) the primary mass flow standard. The mass flow standard uses a balance (weigh scale) to measure the rate of change of mass accumulating in a collection beaker. See Figure 1.

2.1 Flow Sources

We used two flow sources. The first was a syringe pump, Braintree Scientific Model 9000-2,¹ that can generate flows up to 22 mL/min when used with a 12.4 mm diameter glass syringe. It operates using a geared-down stepper motor, that advances a screw which then pushes (or retracts) the syringe piston into (or out of) the syringe barrel. The accuracy of the flow is determined largely by the accuracy of the measured diameter of the piston and barrel and whether there is leakage around the glass piston/barrel annulus. The syringe pump delivers a set volume/time, dV/dt , and the pressure in the line reacts to any changes in flow impedance. In the present work we did not measure the leakage around the piston.

The 2nd flow source was an elevated water reservoir that generates flows based on its elevation in the earth's gravitational field relative to the elevation of the liquid meniscus in the beaker down-stream. At present, we are using a vertical translational stage to elevate the reservoir. The stage has a range, $\Delta h = 15$ cm and can generate pressure differences in water of $\rho g \Delta h \approx 1700$ Pa. The resulting flow then depends on this pressure difference divided by the flow impedance between the up-stream and down-stream menisci. The thermal flow meters used in the present study have capillary restrictions that allow their maximum flows to be reached with this pressure difference. We plan to increase this pressure range an order of magnitude to 17 kPa by using a translation stage with $\Delta h = 150$ cm.

The syringe-pump source is capable of generating much greater pressures than the gravity-feed source and flow is undeterred by the presence of bubbles when using the syringe pump.

In contrast, bubbles are a recurring problem while using the gravity-feed source. A bubble can block the tubing; in particular it can block the capillary inside the smaller-range meter (estimated radius 75 μm). We estimate that the pressure needed for bending the gas-liquid interface

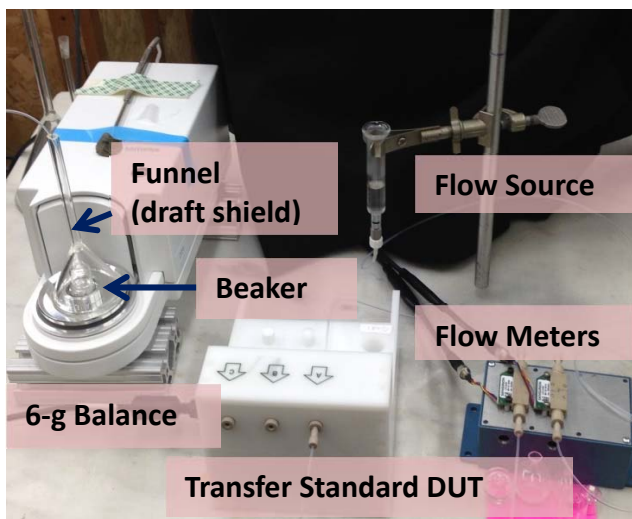


Fig.1. The NIST flow standard micro-Balance is shown on the left in this figure. The elevated reservoir with distilled water is shown with two thermal flow sensors in series with the transfer standard.

¹ In order to describe materials and procedures adequately, it is occasionally necessary to identify commercial products by manufacturers' name or label. In no instance does such identification imply endorsement by the National Institute of Standards and Technology, nor does it imply that the particular product or equipment is necessarily the best available for the purpose.

enough to go through the capillary is about 1600 Pa. Our 15 cm vertical stage was capable of generating a pressure of 1700 Pa. This was marginal and often our flows became blocked in spite of our efforts. Although a 150 cm motorized stage will be used in the next generation, it will be important to keep bubbles out of the system as much as possible.

To this end, we tried both reverse-osmosis and distilled water. This did not guarantee that bubbles of dissolved air didn't form. Both water types seemed equally susceptible to bubbles. Because of this we prepared the reverse-osmosis and distilled water by heating it and bubbling helium gas through it. Even so, the reservoir was open to the air and eventually absorbed air which then re-emerged as bubbles under some circumstances.

2.2 Balance, Beaker, Funnel, and Pipette

For the flow reference standard we are using a weigh scale (balance) configured to take successive mass readings, $m(t_i)$ and $m(t_{i+1})$. The approximate mass flow is then the difference between two readings divided by the time interval, $\Delta m/\Delta t$. We used two balances in these experiments, one was a 200 g balance with sensitivity 0.1 mg (Mettler AE200); the second was a 6 g balance shown in Figure 1, with sensitivity 0.1 μ g (Sartorius CCE6)¹.

A glass beaker made in NIST's glass shop collected water on the weigh scale. A 0.79(2) mm outside-diameter glass pipette formed the final part of the tubing and was inserted into the beaker and penetrated the meniscus.² All components in the flow circuit were connected by 1 mm diameter polyethylene tubing.

The draft shields supplied by the balance manufacturers were not designed to allow tubes to be inserted for access to the weighing pan. We removed these shields and instead used inverted glass funnels of different sizes as temporary substitutes. The inverted funnel served two purposes; 1) as a replacement draft shield and 2) as a tubing support structure so that the pipettes were properly located and did not touch the glass beaker. In the next phase of the project, a translational stage for the pipette will be used to support and position it.

2.3 Flow Meters

We used two commercial thermal-flow meters for most of the validation studies that led to the present data. A third meter (hereafter referred to as the device under test (DUT), Fluigent, Model Flowell 3015002)¹ was a thermal flow meter with a full scale flow of 7.6 μ L/min, which was hand carried to DTI and METAS for an informal comparison.

3. Working Equations for Flow

The mass flow equation for the standard is based on the change in the mass of the liquid collected in the beaker divided by the time interval between mass measurements with corrections for buoyancy, evaporation, and surface tension effects. The equation for volumetric flow is:

$$Q_{Std} \rho_{Liq} = F_{Std} \equiv \frac{dm_{Liq}}{dt} \approx \frac{m_{Read}(t_2) - m_{Read}(t_1)}{t_2 - t_1} \left[\frac{1 - \frac{\rho_{Air}}{\rho_{Std}}}{1 - \frac{\rho_{Air}}{\rho_{Liq}}} - \frac{A_{pipette}}{A_{beaker} - A_{pipette}} \right] - \frac{dm_{zero}(t)}{dt} + \frac{dm_{Evap}(t)}{dt} + \frac{C_{pipette}}{g} \frac{d}{dt} (\gamma(t) \cos \theta(t)) , \quad \text{Eq. 1}$$

² Quantities in parentheses denote estimated standard uncertainties in the preceding digit.

where Q_{Std} is the volumetric flow, $F_{Std}(=dm_{Liq}/dt)$ is the mass flow of the standard and equal to the mass flow from the pipette into the receiving beaker. ρ_{Liq} is the density of the calibration liquid at the meter under test, and $m_{Read}(t)$ is the mass value read by the balance at time t . The factor in the square brackets in Eq. 1 is the scale factor, S , which is a function of the air density ρ_{Air} , the liquid density, ρ_{Liq} , and the density of the masses used to calibrate the balance, ρ_{Std} , typically = 8.0 g/cm³. S is also a function of the area of the pipette $A_{pipette}$, and the cross sectional area of the beaker at the height of the meniscus, A_{beaker} .

The first term within the brackets is a buoyancy correction term for measuring a mass with density that is not equal to the reference masses used to calibrate the balance. The second term within the inner brackets accounts for water displacement by the partially submerged pipette and is necessary because the pipette causes the water level in the beaker to rise faster than it otherwise would if the pipette did not penetrate the meniscus.

dm_{Zero}/dt is the drift of the balance and dm_{Evap}/dt is the evaporation rate of the water from the receiving beaker. The last term in Eq. 1 includes $C_{Pipette}$, the circumference of the pipette, g the local gravitational acceleration, γ the surface tension of the air/water interface, and θ the contact angle of the water/pipette(glass) interface. The last term in Eq. 1 is meant to include not only the rate of change in the surface tension but also the possibly-changing contact angle. The flow equations in references [4, 5] include additional terms to account for changes in air and liquid density changes due to temperature changes in the interval between t_1 and t_2 .

4. Experiments

4.1 Evaluation of Flow Sources

Our first measurements in the flow range 0.25 $\mu\text{L}/\text{min}$ to 100 $\mu\text{L}/\text{min}$ were made using the syringe pump as the flow source with the effluent flowing directly into a beaker on the 200 g balance. The syringe pump delivered a user-specified volume of liquid per unit time. The syringe piston diameter was measured with a micrometer and was 12.44(2) mm in diameter. The inner diameter of the close-fitting cylinder (glass) was not measured. (This will be done before the micro flow calibration service is up and running. A fall-rate method for determining crevice widths in piston gages could be applied here.)⁶ The diameter of the syringe (in the present case the diameter of the piston) was entered as an input parameter to the syringe-pump firmware; then the volumetric flow on the syringe pump was selected.

We compared the mass readings per unit time from the 200 g balance with the selected volumetric flow. See Figure 2. In

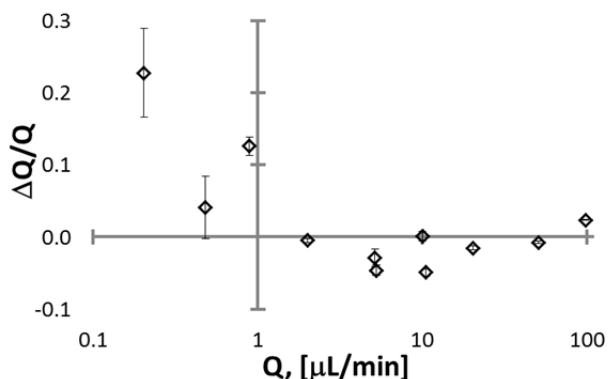


Fig.2. Relative deviations of the flow generated by the syringe pump vs the flow standard. The diamonds indicate differences between the syringe-pump settings from measured mass flow readings from a 200 g balance with resolution 0.1 mg. The mass flows have been converted to volume flow with conversion factor using water density of 0.998 g/cm³. Temperatures (≈ 22 °C) were not monitored closely for this work. Above 2 $\mu\text{L}/\text{min}$, the syringe pump and the balance agree to within 5%. Below 2 $\mu\text{L}/\text{min}$, the error increases for unknown reasons, possibly syringe leakage or an error in the assumed evaporation rate.

one trial we inserted a flow meter (54 $\mu\text{L}/\text{min}$ full scale flow) in the line between the pump and balance to get an additional comparison. Volumetric flow settings of 15 $\mu\text{L}/\text{min}$ generated peak flows greater than the 54 $\mu\text{L}/\text{min}$. The syringe pump will work for larger range meters but will have to be modified for the smaller range meters that we used here. This will be done by using smaller diameter syringes or by inserting ballast after the syringe pump and before the first meter to dampen the pulses. In the meantime, we removed the meter from the circuit and directly compared the syringe pump set point flows and gravimetric flow measurements made with the 200 g balance.

The syringe-pump flow settings, dV/dt , are compared with the mass differences measured by the 200 g balance per unit time in Fig. 2. Buoyancy and pipette displacement corrections were made and mass flows were converted to volume flows using an approximate value for the density of water 0.998 g/cm^3 . Mass readings were made every 60.0(0.4) s. Evaporation rates were previously measured for this beaker and used to correct the mass readings. Because the balance resolution was 0.1 mg, 20 h long collection times were used to produce significant mass changes. In future tests using the 6 g microbalance, evaporation rates will be determined orders of magnitude faster than with the 200 g balance.

Our second flow source was a small 5 mL reservoir attached to a vertical-motorized stage capable of 15 cm height change to generate the pressure and subsequent flow in the tubing. The flow source that used an elevated reservoir provides a non-pulsatile pressure to generate the flow and hence the meters did not saturate during the measurements.

4.2 Evaporation

Water evaporation from the beaker or water leakage past the piston/barrel crevice are likely responsible for the discrepancy in Fig. 2 at the low flows. Because the evaporation measurements took many hours with the 200 g balance, the evaporation was not carefully measured after the flow measurements were made. If the evaporation from the beaker were as high as 0.07 mg/min instead of 0.04 mg/min, the value used to correct the data, the deviations at the low flow end of the figure would be smaller.

Once the 6 g balance and gravimetric flow generator were up and running, we focused our attention on them rather than the 200 g balance and syringe pump. The evaporation was measured in one instance with the 6 g balance by setting up a back flow and siphoning water from the beaker back into the reservoir. See Figs. 3a-3d. As the meniscus in the beaker moved down, the liquid connection to the pipette broke. After the meniscus ruptured, the mass changes per unit time, $\Delta m/\Delta t$, had only one contribution; *i.e.* from evaporation. This value can be read from the red curve in Fig. 3a on the right which in this case, was about 0.041(6) mg/min.

At the Danish Technological Institute, evaporation is controlled by covering the water meniscus with a thin layer of mineral oil. This reduces the evaporation rate by more than an order of magnitude [4]. At METAS the evaporation is controlled by a highly engineered receptacle that contains a porous glass frit. The evaporation is limited by the very small access hole and the high-humidity environment (evaporation trap) surrounding the receptacle [5]. With the technique shown in Fig. 3a we are able to measure the evaporation rate in situ.

4.3 Surface Tension

Figure 3a not only gives information about the evaporation (red curve after the meniscus break) but also about the surface tension. See the discontinuity in the black curve at $t \sim 3$ h. The flow in this case was small enough so that near the extremum in Fig. 3c, we were able to measure about 4 points at intervals of 15 s between the extremum and the point of instability when the meniscus broke. See Fig. 3a-3d. The surface tension can be estimated from the mass measurement discontinuity as the meniscus ruptures; $\gamma = g^* \Delta m / C_{\text{Pipette}} \approx 56$ mN/m. This value is a first order estimate and is a bit low for distilled water and may indicate the presence of some contamination.

Surface tension causes noise in the mass measurement if the water does not completely wet (or de-wet) the glass pipette as the level of water in the beaker changes. If the water is contacting the pipette with an ideal contact angle of zero (or 180°), then the upward force is constant as the beaker fills and the meniscus moves up the pipette. However if the water does not completely wet the pipette but instead contacts it at a finite contact angle, then there is a likelihood that the meniscus will stick and then slip to a new location on the pipette as the beaker fills, thus creating an irregular force on the balance. Evidence of this “noise” can be seen in the red curve, dm/dt , in Fig. 3a. On the left the noise is ≈ 0.06 mg/min; on the right the noise is ≈ 0.003 mg/min. The increased noise on the left is most likely caused by the stick-slip of the meniscus on the pipette. The noise evidenced in Fig. 3a on the left is much smaller than other cases we have seen which have been on the order of 0.15

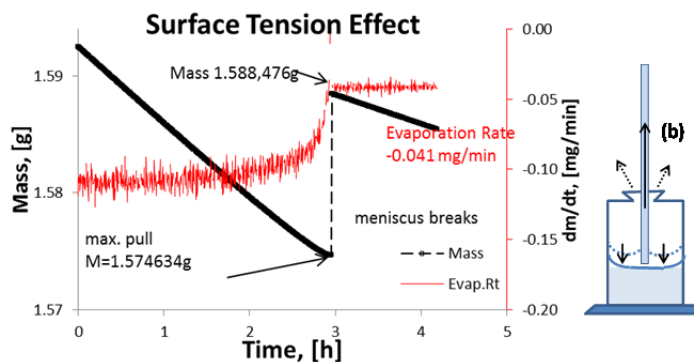


Fig.3a. Surface Tension Effect. The black symbols show the mass record vs time. A reverse flow has been set up; fluid is being siphoned out of the collection beaker back into the reservoir. On the left, before the meniscus separation, the slope has three contributions: 1) the water being siphoned out; 2) the mass loss from evaporation; and 3) the changing pull of the capillary. The total mass flow out of the beaker, $\Delta m / \Delta t$, is shown in red. After the separation the red line displays the evaporation rate. The difference in mass before and after the break is a measure of the surface tension; $\gamma = g^* \Delta m / C_{\text{Pipette}}$. **Fig. 3b.** The cartoon on the right depicts the partially-filled collection beaker and pipette; the dotted blue line indicates the meniscus before the separation; the solid blue line indicates the meniscus after the separation.

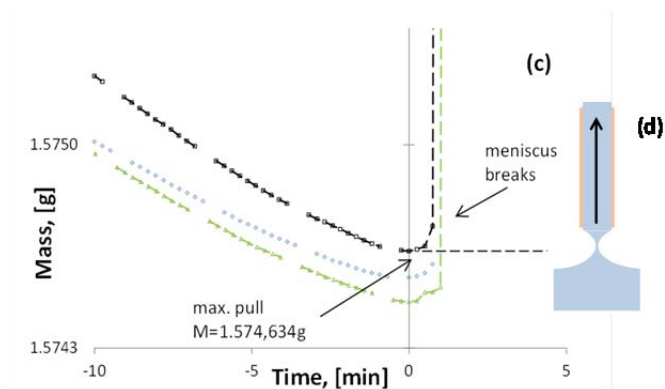


Fig.3c. The Surface Tension Effect Detail. The black symbols show a detail of Fig 2a near the region of maximum upward pull (mass minimum) before the meniscus breaks. Data were taken at intervals of 15 s. The runs were repeated twice more (blue and green symbols). The differences between the extrema of the runs indicate a possible shift of the pipette between the three runs. **Fig. 3d** shows a cartoon of the meniscus at the end of the pipette just before the meniscus breaks.

mg/min; the case considered in the uncertainty analysis.

At METAS the surface tension contribution is held constant because there is no moving interface between the pipette and the collection beaker. A stationary porous glass frit receptacle takes the place of the moving air/water interface [5]. At DTI the surface tension contribution is reduced by using a layer of mineral oil covering the water. Their steel pipettes are specially treated to become oleo-phobic [4].

In the present work, the surface tension and the noise associated with the contact angle are the most significant errors and we are exploring the METAS and the DTI techniques for reducing the noise caused by this effect.

4.4 Timing Issues

There are unresolved timing issues with the balances that we are presently working through. It took us some time to expose this issue, as it was comparable to possible surface-tension/pipette-wetting issues and the two contributions seemed inseparable for a time. We eventually hit on the following test to separate the two effects. We removed the pipette and beaker and replaced them with a small paper towel, $m_{\text{Towel}} \approx 5 \text{ mg}$, area $\approx 1 \text{ cm}^2$, on the weighing pan of the microbalance. Then we soaked the towel with acetone, $m_{\text{Total}}(t=0) \approx 0.1 \text{ g}$. The acetone evaporated within 6 minutes and generated mass changes comparable to some of the flows we were trying to measure. See Fig. 4.

The inset in Figure 4 shows a close-up section at $t \approx 1 \text{ min}$. The “jogs” in the data are clearly apparent and amount to about a 0.25 s error in timing. With more attention to the LABVIEW¹ programming and the communication code, we believe that we can reduce the timing errors to a few milliseconds, which has been done at both DTI and METAS.

5. Informal Comparison Results

A preliminary calibration in our facility was within 3 % of two unofficial calibrations one from the Danish Technological Institute in Aarhus, Denmark, and the other from the Swiss Feral Institute of Metrology in Bern, Switzerland at flows down to $2 \mu\text{L}/\text{min}$. (See Figures 5 and 6.) The DTI and METAS calibrations are unofficial and were conducted on a very compressed time schedule and do not represent the accuracy achievable by these labs.

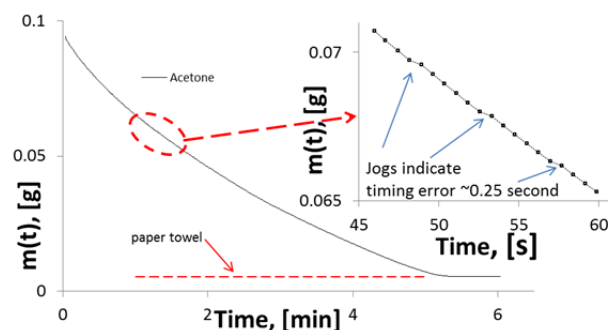


Fig.4 Mass Record vs Time (Acetone Evaporation). This plot shows mass as a function of time taken from the 6 g balance in which a 1 cm^2 paper-towel segment is resting on the weighing pan. The paper towel was initially soaked with acetone that immediately started to evaporate. The mass changes per minute are comparable to the flows from a pipette into a small beaker that we were trying to measure. The data circled in red is shown in the inset on an expanded scale.

Inset (Detail of the region at $t \approx 1 \text{ min}$.) This magnified segment shows three “jogs” in the data and they indicate a timing error of 0.25 s that we are working to resolve. The equivalent mass error for this timing error at the “flow” equivalent [$\approx 25 \text{ mg}/\text{min}$] would be about 0.130 mg. We believe this is correctable with modifications to the measurement software. (See Refs. 4&5).

Figure 5 shows a comparison of the DTI and METAS calibrations of the DUT. The two laboratories agree with each other within 2 % and within their uncertainty specifications. The error bars are one standard deviation of the repeated measurements made at each flow set point. The results also suggest that the DUT is stable.

Figure 6 shows a comparison of the NIST calibration results vs. the average of the other two laboratories. Our data are within 3 % of the unofficial calibrations by DTI and METAS For $Q > 2 \mu\text{L}/\text{min}$.

For flows less than $1 \mu\text{L}/\text{min}$ the NIST results are high compared with the DTI and METAS calibrations. Future repetitions with a tighter control of our timing errors and surface tension should determine whether this difference is real or not.

6. Uncertainty Analysis

Here we examine the terms in Eq. 1 and estimate the contributions to the uncertainty of F_{std} , the mass effluent at the end of the pipette. At the end of the analysis we also calculate the uncertainty of volumetric flow. We organize the uncertainties into four groups, 1) the mass balance uncertainty, 2) timing uncertainty, 3) uncertainty of quantities that affect the scale factor S of the mass-flow measurement and 4) those that affect the flow offset, F_{offset} .

$$F_{\text{Std}} \approx \frac{\Delta m_{\text{Bal}}}{\Delta t} S + F_{\text{Offset}} \quad \text{Eq. 2}$$

S is a function of ρ_{Air} , ρ_{Std} , ρ_{Liq} , A_{pipette} and A_{beaker} . F_{Offset} is a function of dm_{zero}/dt , dm_{Evap}/dt , C_{pipette} , g , $d\gamma(t)/dt$ and $d\theta(t)/dt$.

6.1 Mass Balance Uncertainties: $u(m_{\text{Bal}})$

The 6 g balance has resolution $0.1 \mu\text{g}$ and a repeatability of $0.15 \mu\text{g}$. Assuming no balance drift, non-linearity, or calibration uncertainty, for two mass measurements, the uncertainty in their difference is: $u(\Delta m) = \sqrt{2} (0.1^2 + 0.15^2)^{1/2} \approx 0.25 \mu\text{g}$. For the present analysis we always take the time interval $t_2 - t_1$ as 1 min, giving an uncertainty due to resolution and repeatability in the flow of $0.25 \mu\text{g}/\text{min}$.

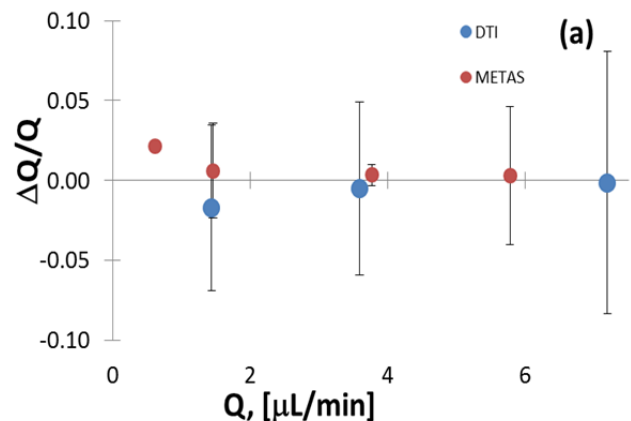


Fig. 5. Relative deviations of two Laboratories from the average fit. Two laboratories show good agreement with each other using the DUT as a transfer gauge. DTI – blue dots; and METAS – red dots.

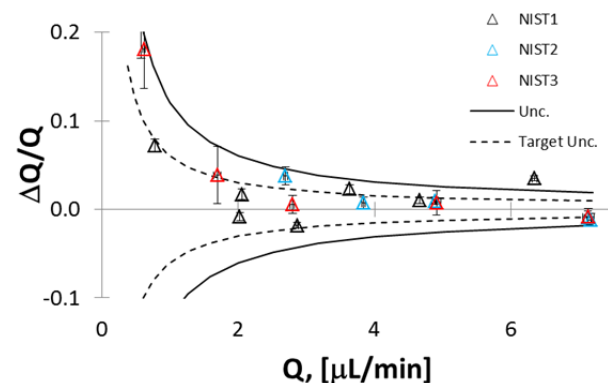


Fig. 6. Relative deviations of NIST from DTI and METAS. Triangles represent deviations of NIST (3 trials) from the average of two laboratories. Solid line represents estimated uncertainties. Dashed line represents target uncertainties.

The balance-zero drift rate, dm_{zero}/dt , is estimated based on the maximum rate of drift observed over a period of 5 days. We will conservatively assume that the maximum zero drift rate during this test (0.16 $\mu\text{g}/\text{min}$) is a standard uncertainty value for this component. Laboratory temperature control is nominally ± 1 K and the balance was not in a temperature-controlled enclosure.

Combining these contributions to the flow uncertainty we have for $u(\Delta m_{Bal})$:

$$\left(\left(\frac{u(\Delta m)}{\Delta t} \right)^2 + \left(\frac{dm_{zero}}{dt} \right)_{Max}^2 \right)^{1/2} = \left(\left(\frac{0.25 \mu\text{g}}{1 \text{ min}} \right)^2 + \left(\frac{0.16 \mu\text{g}}{\text{min}} \right)^2 \right)^{1/2} = 0.30 \mu\text{g}/\text{min} \quad . \quad \text{Eq.3}$$

6.2 Timing Uncertainties $u(t_2-t_1)$

Only recently were we able to separate micro balance timing issues from surface tension issues as discussed in section 4.4. The timing uncertainty will be addressed and reduced in future measurements.

For the NIST data in Fig. 6 the timing uncertainty was on the order of 0.25 s. This leads to an uncertainty in the flow of 0.4 % for an integration time of 1 min. This is a significant scale error, but will be reduced by almost 2 orders of magnitude in future work. The uncertainty in the mass flow due to timing uncertainty is:

$$u(F_{Std}(\Delta t)) \approx \frac{\Delta m_{Bal}}{(\Delta t)^2} \times S \times u(\Delta t) \approx F_{Std} \times 1 \times \frac{u(\Delta t)}{\Delta t} \approx F_{Std} \times 0.004 \quad . \quad \text{Eq. 4}$$

6.3 Scale-Factor Uncertainties $u(S)$

The scale factor in Eq. 1 (the terms in brackets) is affected by ρ_{Air} , ρ_{Liq} , $A_{pipette}$ and A_{beaker} .

Air and Liquid density: The scale sensitivities to liquid and air densities are:

$$\frac{dS}{d\rho_{Air}} \approx \frac{-1}{\rho_{Std}} + \frac{1}{\rho_{Liq}} \approx 0.0009 \frac{1}{\text{kg}/\text{m}^3} \quad ; \quad \text{Eq. 5a}$$

$$\text{and} \quad \frac{dS}{d\rho_{Liq}} \approx \frac{-\rho_{Air}}{\rho_{Liq}^2} \approx 1.2 \times 10^{-6} \frac{1}{\text{kg}/\text{m}^3} \quad . \quad \text{Eq. 5b}$$

Estimating $u(\rho_{Air}) = 0.012 \text{ kg}/\text{m}^3$ and $u(\rho_{Liq}) = 1 \text{ kg}/\text{m}^3$, we get $(dS/d\rho_{Air}) u(\rho_{Air}) \approx 11 \times 10^{-6}$, and $(dS/d\rho_{Liq}) u(\rho_{Liq}) \approx 1.2 \times 10^{-6}$.

Pipette and Beaker Area: In Eq. 1 the scale sensitivity to pipette cross-sectional area is:

$$\frac{dS}{dA_{pipette}} \approx \frac{-1}{A_{beaker} - A_{pipette}} - \frac{A_{pipette}}{(A_{beaker} - A_{pipette})^2} \quad , \quad \text{Eq. 6a}$$

and the scale sensitivity to beaker cross-sectional area is:

$$\frac{dS}{dA_{Beaker}} \approx \frac{A_{pipette}}{(A_{beaker} - A_{pipette})^2} \quad . \quad \text{Eq. 6b}$$

The pipette used here had outer diameter $D_{\text{pipette}}=0.79(1)$ mm, the pipette circumference was $C_{\text{pipette}}= \pi D_{\text{pipette}} =2.47(3)$ mm, and the cross sectional area was $A_{\text{pipette}}=\pi D_{\text{pipette}}^2/4 =0.487(12)$ mm². The diameter of the beaker was 15.67(8) mm and the area of the beaker, was 193(2) mm².

The quadrature sum of the two contributions to the scale uncertainty above, $u(S(A_{\text{pipette}}))$ and $u(S(A_{\text{Beaker}}))$ is:

$$u(S) \sim \left[\left(\frac{1}{A_{\text{beaker}} - A_{\text{pipette}}} + \frac{A_{\text{pipette}}}{(A_{\text{beaker}} - A_{\text{pipette}})^2} \right)^2 u^2(A_{\text{pipette}}) + \left(\frac{A_{\text{pipette}} u(A_{\text{beaker}})}{(A_{\text{beaker}} - A_{\text{pipette}})^2} \right)^2 \right]^{1/2}, \quad \text{Eq. 7a}$$

$$\sim \frac{1}{A_{\text{beaker}} - A_{\text{pipette}}} \left[\left(\frac{A_{\text{beaker}}}{A_{\text{beaker}} - A_{\text{pipette}}} \right)^2 u^2(A_{\text{pipette}}) + \left(\frac{A_{\text{pipette}}}{A_{\text{beaker}} - A_{\text{pipette}}} \right)^2 u^2(A_{\text{beaker}}) \right]^{1/2}, \quad \text{Eq. 7b}$$

$$\sim \frac{1}{(193 - 0.487) \text{mm}^2} \left[\left(\frac{193 \text{mm}^2}{(193 - 0.487) \text{mm}^2} \right)^2 (0.012 \text{mm}^2)^2 + \left(\frac{0.487 \text{mm}^2}{(193 - 0.487) \text{mm}^2} \right)^2 (2 \text{mm}^2)^2 \right]^{1/2}, \quad \text{Eq. 7c}$$

$$\sim 60 \times 10^{-6} \quad . \quad \text{Eq. 7d}$$

The quadrature sum of the scale factor uncertainties is:

$$u(S) \sim (11^2 + 1.2^2 + 60^2)^{1/2} \times 10^{-6} \approx 61 \times 10^{-6} \quad . \quad \text{Eq. 8}$$

6.4 Offset Uncertainties: $u(F_{\text{Offset}})$

Component uncertainties that contribute to an offset error in Eq. 1 are: dm_{Evap}/dt , $d\gamma/dt$, $d\theta/dt$.

Evaporation Rate: dm_{Evap}/dt

The evaporation rate of water from the beaker with inverted funnel in place is shown in Fig. 3a, and is ≈ 41.2 $\mu\text{g}/\text{min}$ with a standard deviation of ± 1.3 $\mu\text{g}/\text{min}$. Repetitions of this measurement on other days yielded a much larger variation of ± 7 $\mu\text{g}/\text{min}$ and this is the value we will use as a standard uncertainty in this analysis. Laboratory humidity was not monitored for these measurements, but will be monitored in the future.

Surface Tension:

The last term in Equation 1 allows not only for a changing surface tension but also for a changing contact angle of the meniscus against the pipette. The surface tension of pure water tension in air is close to 0.070 N/m. Reverse osmosis water was used in these measurements. The water was heated and bubbled with helium for several hours to remove air impurities. For these measurements the rate of change of the surface tension may be important. More importantly, however, is the change of the contact angle over time, which is not under control at present. We are investigating the DTI technique of using a specially coated pipette. We are also investigating the METAS technique of using a glass frit receptacle which avoids the moving water/glass interface.

We assume that the uncertainty contribution from changing surface tension is negligible but that the uncertainty contribution from changing contact angle is not. Postulating a 0.1 % change in surface tension, an average contact angle $\langle \theta \rangle \approx 5^\circ$ with random changes in contact angle of $|\delta\theta| \approx 1^\circ$ between two measurements 1 min apart yields an estimated change in the mass reading of:

$$\Delta m \approx \frac{C_{\text{pipette}}}{g} \left(\left(\cos \theta \frac{d\gamma}{dt} \right)^2 + \left(\gamma \sin \theta \frac{d\theta}{dt} \right)^2 \right)^{1/2} \times 1 \text{ min} \quad , \quad \text{Eq. 9a}$$

$$\approx \frac{0.00247 \text{ m}}{9.8 \frac{\text{m}}{\text{s}^2}} \left(\left(0.96 \times 56 \times 10^{-6} \frac{\text{N}}{\text{min}} \right)^2 + \left(0.056 \left(\frac{\text{N}}{\text{m}} \right) 0.26 \frac{1^\circ \pi}{180^\circ \text{ min}} \right)^2 \right)^{1/2} \times 1 \text{ min} \quad , \quad \text{Eq. 9b}$$

$$\approx 65 \mu\text{g} \quad . \quad \text{Eq. 9c}$$

For a measurement interval of 1 min this leads to a flow uncertainty 65 $\mu\text{g}/\text{min}$, and is the largest contributor to the offset uncertainty.

The quadrature sum of the flow-offset uncertainties is:

$$u(F_{\text{Offset}}) \approx \frac{(7^2 + 65^2)^{0.5} \mu\text{g}}{\text{min}} \approx 65 \mu\text{g}/\text{min} \quad . \quad \text{Eq. 10}$$

6.5 Total Uncertainty of Flow:

The total uncertainty of the standard's mass flow, $u(F_{\text{Std}})$ in Eq. 1 is:

$$u(F_{\text{Std}}) \approx \left[\left(\frac{u(\Delta m)}{\Delta t} \right)^2 + \left(\frac{dm_{\text{Zero}}}{dt} \right)^2 + \left(\frac{\Delta m}{(\Delta t)^2} \right)^2 u^2(\Delta t) + \left(\frac{\Delta m_{\text{Std}}}{\Delta t} \right)^2 u^2(S) + u^2(F_{\text{Offset}}) \right]^{1/2} \quad , \quad \text{Eq. 11}$$

and the relative uncertainty of the mass flow is:

$$\frac{u(F_{\text{Std}})}{F_{\text{Std}}} \approx \left[\frac{0.25^2 (\mu\text{g}/\text{min})^2}{F_{\text{Std}}^2} + \frac{0.16^2 (\mu\text{g}/\text{min})^2}{F_{\text{Std}}^2} + (4 \times 10^{-3})^2 + (61 \times 10^{-6})^2 + \frac{65^2 (\mu\text{g}/\text{min})^2}{F_{\text{Std}}^2} \right]^{1/2} \quad . \quad \text{Eq. 12}$$

The standard uncertainty of the volumetric flow includes the uncertainty in the liquid density (0.1 %):

$$\frac{u(Q)}{Q} = Q \frac{u(\rho_{\text{Liq}})}{\rho_{\text{Liq}}} + \frac{1}{\rho_{\text{Liq}}} u(F_{\text{Std}}) \approx 0.001 Q + \frac{u(F_{\text{Std}})}{998 \text{ kg}/\text{m}^3} \quad . \quad \text{Eq. 13}$$

We converted this uncertainty to a 95 % confidence level by multiplying by a coverage factor of 2 and it is plotted as a solid line in Fig. 6. At 1 $\mu\text{L}/\text{min}$ and 5 $\mu\text{L}/\text{min}$, Equation 12 gives $k = 2$ uncertainty of 12 % and 2.5 % respectively for the present iteration of the flow standard. Surface tension effects dominate the uncertainty at low flow. At high flows timing uncertainties are dominant. We will reduce both of these uncertainties in future iterations of the flow standard. As we extend the flow standard to lower flows, we expect evaporation to be a significant uncertainty component.

7. Discussion

The FMG at NIST has progressed in its development of a micro flow standard that spans the range 1 mL/min down to 0.25 μ L/min. We have used two types of flow sources, a syringe pump and a gravimetric pressure head together with two mass balances (200 g and 6 g). Our present uncertainty analysis indicates that we can measure flows down to 2 μ L/min with uncertainty of 6 % ($k = 2$) or better, but our comparison results are better (3 %). We are in the process of solving a timing issue with the balances and surface tension/wetting issues between the pipette and the water. The timing issue will be solved by improving the communication protocol with the balance. We plan to improve the pipette wetting uncertainties by following the examples of other laboratories, i.e. surface treatment of the pipette or a porous frit receiver. Once these two problems are solved, we expect to acquire data at the rate of 2.5 Hz with an estimated uncertainty of 3 % down to 2 μ L/min. We also plan to place the standard in an enclosure and better control the environmental conditions surrounding the apparatus.

In future work, the FMG is planning to purchase or design and build other micro flow meters for flows down to 10 nL/min or less with an objective to improve the physical models, conduct research on small liquid flows, and develop best practices for measuring micro flows.

8. Acknowledgements

We thank Drs. John Frederiksen, Anders Niemann of the Danish Technological Institute and Drs. Marc de Huu and Hugo Bissig of METAS for their hospitality and for allowing us to use results that we obtained from them under a tight schedule that we imposed on them. We thank Dr. Steve Hudson at NIST for his help and for the loan of a transfer flow meter. We thank Iosif Shinder and Jim Filla at NIST, and Morton K. Rasmussen at DTI for suggestions on resolving our timing issues.

9. References

- ¹ K.H. Knight, F.M. Brand, A.S. Mchaourab, and G.Veneziano, "Implantable Intracathal Pumps for Chronic Pain; Highlights and Updates", *Croat Med. J.*, **48**(1):22-34, Feb, 2007.
- ² S.M. Hayek, T.R. Deer, J.E. Pope, S.J. Panchal and V.P. Patel; "Intrathecal Therapy for Cancer and Non-Cancer Pain", *Pain Physician*, **14**, 219-248, 2011.
- ³ L. Greenemeier, "Exotic Micropumps and Gels Offer Hope for Hearing Disorders"; *Scientific American*, Mar. 15, 2015.
- ⁴ C. Melvad and J. Frederiksen, "The Progress of Gravimetric Primary Standards for Liquid Flow Calibration at the Danish Technological Institute from 500 m³/h to 1E-9 m³/h", *Proceedings FLOMEKO*, Paris, Sept. 24-26, 2013.
- ⁵ H. Bissig, M. Tschannen, M. de Huu, "Micro Flow Facility for Traceability in Steady and Pulsating Flow", *J. Flow Meas. and Instr.*, 2014, in press, <http://dx.doi.org/10.1016/j.flowmeasinst.2014.11.008>
- ⁶ K. Jain, W. Bowers, and J.W. Schmidt, "Primary Dead-Weight Tester for Pressures (0.05-1.0) MPa", *J. Res. Natl. Inst. Stand. Technol.* **108**, 135-145, 2003; Eq. (19).